Excitations, order parameters, and phase diagram of solid deuterium at megabar pressures

Lijing Cui, Nancy H. Chen, and Isaac F. Silvera
Lyman Laboratory of Physics, Harvard University, Cambridge, Massachusetts 02138
(Received 17 January 1995)

In recent infrared experiments on solid *ortho*-deuterium a number of IR-active modes were observed in the various high-pressure phases. We have performed a group-theoretical analysis of IR and Raman activity for the vibrational modes of proposed space groups to aid in determining the structures of the various phases. From a comparison of the theoretical analysis with experimental results, candidate structures for the various phases are selected. The best candidates have underlying molecular centers which form hcp lattices in both the broken-symmetry phase (BSP) and the deuterium-A (D-A) phases; the molecules in each phase are orientationally ordered along crystalline directions not coinciding with the *c* axis. The hcp-*c* structure has been excluded. We have also analyzed the mode frequencies and integrated intensities in these phases to determine the order parameters for the structures. From the temperature dependence of the order parameters a determination of the order of the phase transition can be made. The D-A phase does not end in a critical point, but rather a triple point with a phase line separating the low pressure phase and the D-A phase, above the triple point. Our results are consistent with a first-order phase transition in crossing from the BSP to the D-A phase and a second-order phase transition from the D-A phase to the low pressure orientationally disordered phase.

I. INTRODUCTION

Solid hydrogen and deuterium have fascinating *P-T* phase diagrams at high pressures as shown in Fig. 1(a) for deuterium (Ref. 1, Cui, Chen, Jeon, and Silvera, hereafter referred to as CCJS) and in Fig. 1(b) for hydrogen and its isotopes. At low pressure and low temperature both *para*-H_2 and *ortho*-D_2 form an hcp lattice with molecules in spherically symmetric states. We shall call this the low-pressure (LP) phase. At a $T=0$ K threshold pressure of about 28 GPa for deuterium,[2] and 110 GPa for hydrogen[3] the ground-state symmetry of the low-pressure phase breaks and molecules become orientationally ordered in a phase called the broken-symmetry phase (BSP). The BSP was first predicted to be of $Pa3$ symmetry,[4] and later was proposed for H_2 to have an hcp-ordered structure.[5] Experimentally, the structure of the BSP is undetermined. At higher pressure, about 150 GPa, hydrogen and deuterium transform into a new phase named the hydrogen-A (H-A) or deuterium-A (D-A) phase, respectively. The H-A and D-A phases have been suspected to be the molecular metallic phases, and have attracted much attention both theoretically and experimentally, which will be discussed below. However, little is known of the microscopic details of this phase; at present the conducting nature of the phase is unknown. It was shown by Lorenzana, Silvera, and Goettel[3] that the H-A phase has orientational order. In this article we use a group-theoretical analysis, along with recent spectroscopic observations to further elucidate the nature and structure of the BSP and D-A phases.

Recent infrared (IR) absorption measurements on solid deuterium by CCJS have shown that the D-A phase line does not terminate at a critical point; a triple point has been observed where the BSP phase line meets the D-A phase line. Above this triple point the D-A phase line continues, but the order of the transition was unknown. Below the triple point the phase transition from the BSP to the D-A phase is a first-order transition characterized by a frequency discontinuity in both the IR and Raman vibrons. The discontinuity in the Raman vibron was used to identify the H-A phase line and the disappearance of the discontinuity was interpreted as evidence for a critical point in hydrogen.[6,7] Silvera[8] pointed out that the existence of the critical point implied that the H-A phase has the same symmetry as the LP phase, i.e., hcp symmetry. Recently, Zallen, Martin, and Natoli[9] observed that the IR absorption identified by Hanfland, Hemley, and Mao[10] in H_2 as a vibron is not allowed in hcp symmetry. However, as pointed out by CCJS such arguments cannot be used for the spectra in the impure (mixed *ortho-para* H_2) crystals studied by Hanfland, Hemley, and Mao. We have studied the IR spectra in pure *ortho*-D_2 crystals and find the D-A phase to be incompatible with hcp symmetry.

We believe that the reported critical point in H_2 is actually a triple point as we observed in D_2. In CCJS and in this article it is shown that the disappearance of the vibron frequency discontinuity is insufficient evidence to identify a critical point. The disappearance of the discontinuity occurs for both hydrogen and deuterium, and was the basis for the identification of a critical point. However, more extensive data, i.e., IR spectra, exist only for deuterium. Measurement of IR spectra in hydrogen should also confirm that the reported critical point is actually a triple point.

The nature of the phase transition from the LP phase to the D-A phase above the triple point is not understood at present. Here, we report results of IR and Raman measurements which suggest that the D-A phase line above the triple point may be a second-order phase transition. We perform a group-theoretical analysis of the IR

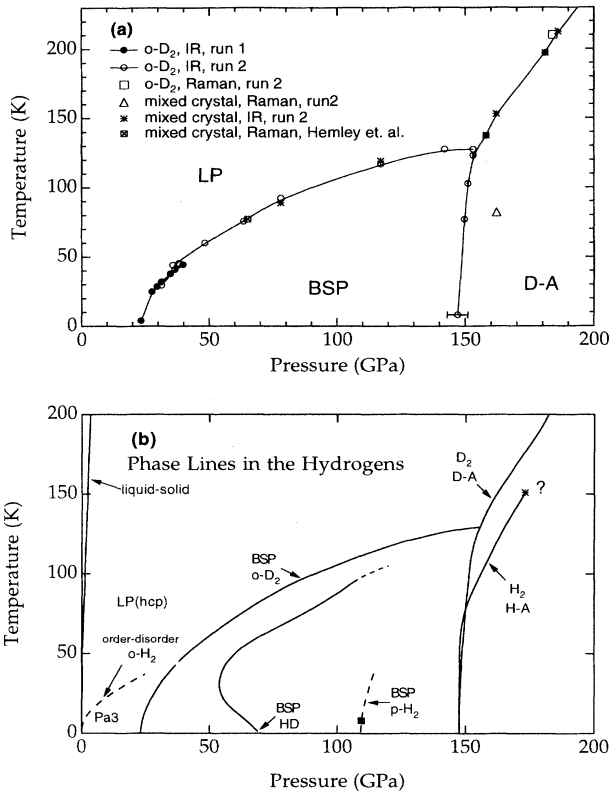

FIG. 1. (a) Various phases of high-pressure solid deuterium identified by IR absorption in this work. Mixed crystals at a given pressure have *o-p* ratios corresponding to the equilibrium value at liquid nitrogen temperature. Raman spectra are also used to determine the D-A phase line, given by the triangle and square. (b) The *P-T* phase diagram of hydrogen and isotopes. Dotted lines indicate expected behavior. The asterisk with a question mark at the end of H-A phase line is the critical point proposed by earlier work (Refs. 6 and 7) based on the disappearance of the discontinuity in the Raman vibron frequencies, as discussed in the text.

and Raman activity of vibrons and phonons for various structures which have been considered for the high-pressure phases of hydrogen. From a comparison of the theoretical analysis with experimental results, candidate structures for the BSP and D-A phases are selected. Based on the selected structures of the various phases we analyze the vibron excitation energies in terms of the intramolecular interaction and the isotropic and anisotropic intermolecular interactions. Taking the dominant anisotropic intermolecular interaction to transform as the electric quadrupole-quadrupole interaction (EQQ), we show that the vibron excitation energies can be used to directly measure the orientational order parameters in both the A and BSP phases.

The hydrogens have two species, resulting in profoundly different properties in the solid. The *ortho-para* identities of hydrogen and deuterium are due to the identical particle symmetry of the nuclei.[11] The most fundamental quantum numbers for identifying the species are the nuclear-spin states ($i=1/2$ for hydrogen and $i=1$ for deuterium). Under particle permutation these are required to combine with the rotational wave functions to have the proper symmetry. For low pressure the rotational wave functions are very well approximated by the spherical harmonics with the free rotor rotational quantum numbers J,m. *Para*-hydrogen (*ortho*-deuterium) corresponds to $I=i_1+i_2=0$, J even ($I=0,2$, J even), whereas *ortho*-hydrogen (*para*-deuterium) corresponds to $I=1$, J odd ($I=1$, J odd). At high pressure J is no longer a good quantum number and the rotational wave functions must be described by even and odd functions which are not spherical harmonics. Conversion to equilibrium mixtures is quite slow and has been studied extensively at low pressure.[11] At high pressure there have been no quantitative studies of the conversion rates. Silvera and Wijngaarden[2] and Lorenzana, Silvera, and Goettel[3] have observed the development of sharp rotational spectra as mixed *ortho-para* samples convert to equilibrium at low temperature, which is attributable to *ortho-para* conversion. The conversion rate is much faster at high pressure than at low pressure. In the current high-pressure work, samples were allowed a minimum of 24 h to convert to equilibrium.

II. THE PHASE DIAGRAM OF *ORTHO*-DEUTERIUM

Based on IR vibron spectra, the phase diagram of *ortho*-D_2 is divided into three regions, as shown in Fig. 1(a). LP is the low-pressure insulating phase with hcp symmetry. In this phase the molecules are in spherically symmetric states (for $J=0$ molecules) or disordered states (for mixed *ortho-para* crystals). Pure *ortho*-H_2 or *para*-D_2 orders into the *Pa*3 structure at low pressures, shown in Fig. 1(b). A group-theoretical analysis has shown that the IR vibron is not an allowed transition for hcp symmetry[12] and this has been confirmed in our experiment with pure *ortho*-D_2. In the BSP phase three distinct IR vib-

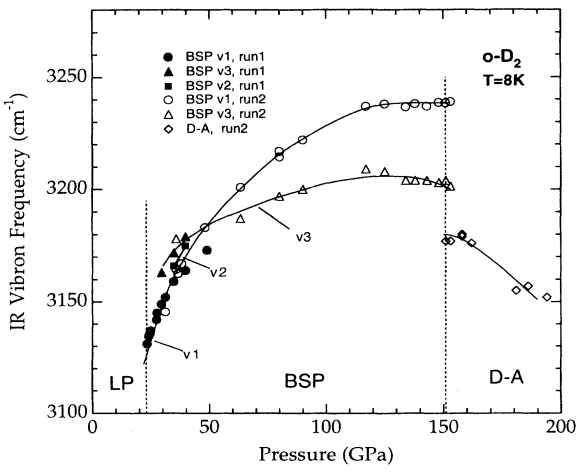

FIG. 2. Pressure dependence of IR vibrons peak frequencies in the various phases of *ortho*-D_2. We believe that the peak represented by the open triangles actually represents vibron $v2$ and $v3$. These peaks were unresolved in run 2 with a thin sample. The solid lines are guides to the eye.

rons are observed. The pressure dependence of their frequencies is shown in Fig. 2. The D-A phase is characterized by a single intense IR vibron whose frequency is about 60 cm^{-1} lower than the vibron of the highest energy in the BSP at the onset pressure of about 150 GPa. The intensity of the D-A vibron absorption line grows rapidly with increasing pressure.

The phase lines are determined by observing changes in the IR spectra from one phase to the other. The Raman spectra are also used to determine the D-A phase transition and the results are shown in Fig. 1(a). At 77 K this transition pressure appears to be about 15 GPa higher than that determined by IR spectra. This pressure difference may be attributable to pressure gradients in the sample, in combination with a difference in relative sensitivity of the IR and Raman measurement techniques. Since the D-A phase line is similar to the H-A phase of hydrogen, it is reasonable to assume that the as yet undetermined nature of these phases is the same for the two isotopes.

III. THEORETICAL ANALYSIS

In this section we discuss the relevant theoretical aspects in analyzing our Raman and IR data. We first carry out the group-theoretical analysis of IR and Raman activity for vibrational modes of various structures which have been proposed for the high-pressure phases. Then we analyze the vibron excitation energies based on the structures selected from the group-theoretical analysis. The vibrational energies depend on both the intra- and intermolecular interactions. In hydrogen the intramolecular interaction is much stronger than the intermolecular interactions and dominates the energy. Finally, we discuss order parameters which characterize the molecular orientational ordering in the various high-pressure phases. The long-range orientational order parameter is defined such that it is nonzero in the ordered phases and becomes zero in the disordered phase. If there is a discontinuity in the order parameter at the transition from an ordered phase to a disordered phase, the transition is first order, whereas a continuous change of the order parameter to zero implies that the transition is second order.

A. Group-theoretical analysis

Hydrogen and deuterium have only one electron per atom, thus it is very difficult to study their high-pressure phases by x-ray diffraction due to the small scattering strength. The difficulties are enhanced at megabar pressures due to the small sample size and the problems in producing single crystals. Up to now the structures of the various high-pressure phases are undetermined. On the other hand, group-theoretical analysis of IR and Raman activity of various vibrational modes can provide a powerful tool to determine the possible structures for the high-pressure phases of hydrogen and deuterium.

It is useful to first review the theoretical pictures of the high-pressure phases. Electronic band-structure calculations have been used to predict stable high-pressure structures of solid hydrogen and metallization pressures. Earlier work by Ramaker, Kumar, and Harris,[13] as well as Friedli and Ashcroft,[14] predicted that hydrogen in the $Pa3$ structure would become a metal in the region of a few hundred GPa. Later Barbee *et al.*[15] showed that a much lower energy high-pressure structure is hcp-*c* with a metallization pressure of 60 GPa. In the hcp-*c* structure the molecular axes are oriented along the *c* axis of the hcp lattice. However, in all of these studies the theoretical method underestimates the metallization pressure. Garcia *et al.*[16] used a modified approach and showed that the hcp-*c* would metallize at 180 GPa. Then, Kaxiras, Broughton, and Hemley[17] and Kaxiras and Broughton[18] showed that there are still lower energy structures on the hcp lattice with molecules rotated away from the *c* axis. These lower symmetry structures have wider energy gaps and thus higher metallization pressures. Recently Nagara and Nakamura[19] enlarged the basis of the hcp lattice to four molecules/unit cell and found a still lower energy space group, $Pca2_1$. This structure is stable until about 300 GPa; above this pressure the rutile structure becomes more stable. However, Surh, Barbee, and Mailhiot[20] considered the effect of vibronic zero-point motion on the $Pca2_1$ structure and found that the hcp-*c* structure becomes the ground state for the insulator-metal transition. Edwards and Ashcroft[21] proposed a class of layered structures for high-density hydrogen. Later, we shall analyze one of these structures with the $Cmca$ space group (four molecules/unit cell). It has also been suggested[22] that the space group $P6_3/m$ could be a stable high-pressure structure. This space group has eight molecules/unit cell and was earlier considered as the stable structure for the low-temperature ordered phase of *ortho*-H_2 or *para*-D_2 at low pressure.[23] The most recent study of crystal structures at high pressure is a quantum Monte Carlo investigation by Natoli, Martin, and Ceperley[24] which includes the zero-point energy directly. They limited their study to hcp lattices with two molecules per unit cell and found the insulating $Pmc2_1$ structure (to arrive at this structure, in Fig. 3 of this paper invert the dashed arrows of the $P2/m$ structure), proposed by Kaxiras and Broughton, to have the lowest energy. [To expedite our analyses, we have identified the space groups of the structures shown by Kaxiras and Broughton. Their Fig. 3(b) is space group $P2/m$ and Fig. 3(e) is $Pmc2_1$.]

For the BSP, earlier work by Raich and Etters[4] predicted the $Pa3$ structure to be the lowest energy structure for pure EQQ interactions. Calculations by Runge *et al.*[15] for a more realistic intermolecular potential predicted that with increasing pressure, *ortho*-D_2 first orders into the $Pa3$ structure and at higher pressure it transforms to an hcp-ordered structure, while *para*-H_2 orders directly into an hcp-ordered structure at high pressure. Experimentally, the structure of the BSP is undetermined.

In Fig. 3 we show the detailed structures of the $Pca2_1$ space group proposed by Nagara and Nakamura[25] and the $P2/m$ space group proposed by Kaxiras and Broughton.[18] For comparison we also show the hcp space group for the LP insulating phase. For all of the three space groups, the molecular centers are on an hcp

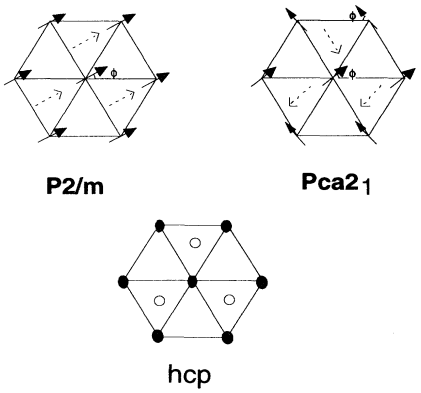

FIG. 3. Illustration of structures: $P2/m$, $Pca2_1$, and hcp. Solid lines represent molecules lying in a c plane and broken ones in the next c plane. Arrows indicate the direction of molecular axes whose direction cosines with the z axis are positive and they do not imply the directions of dipoles. In the $P2/m$ structure all molecules have the same orientation with $(\theta,\phi)=(60°,30°)$ (Ref. 18). In the $Pca2_1$ structure, molecules take one of the four orientations. The polar and azimuthal angles of the molecular orientation at the origin are $(\theta,\phi)=(59.3°,37.6°)$, in accordance with Ref. 19. In the hcp-c structure, the molecular orientation is perpendicular to the plane.

lattice. In the $P2/m$ structure the molecules are rotated away from the c axis of the hcp lattice by a polar angle $\pi/3$. In the $Pca2_1$ structure, the molecules orient in one of four different directions, and their polar and azimuthal angles are given in Fig. 3. The $P2/m$ and the hcp structures have two molecules per unit cell; the $Pca2_1$ structure has four molecules per unit cell.

To aid in determining the structures of the various high-pressure phases we have carried out a group-theoretical analysis of IR and Raman activity of vibrational modes for the various structures proposed for the high-pressure phases. The results of this analysis, the number of allowed vibrational modes and their irreducible representations are given in Table I. Note that for space groups with inversion symmetry, Raman-active modes are those with even irreducible representations which are denoted by the subscript g, and IR active modes are those with odd irreducible representations which are denoted by the subscript u. For space groups without inversion symmetry, modes can be Raman and IR active simultaneously. The results in Table I are valid for solids with translational symmetry and thus are in principle applicable only to pure o-D_2 (p-H_2) crystals. The experimentally observed number of IR and Raman modes are shown for *ortho*-D_2 at the bottom of the table. Note that in earlier work at low pressure an IR vibron

TABLE I. The group theoretically allowed IR and Raman modes corresponding to proposed high-pressure space groups of the solid hydrogens. The numbers in brackets are the total number of distinct allowed modes. Asterisks indicate that the irreducible representation B_1 (or B_{1g}) is interchangeable with B_2 (or B_{2g}) due to the definition of the 180° rotation axes in the corresponding space groups. The references in column 6 are the theoretical work in which the various structures were proposed. The number of observed IR and Raman vibrons given at the bottom are from the present work for *ortho*-D_2. The results for the Raman phonons are from the literature for both D_2 and H_2. Measurements in Ref. 37 were made in mixed crystals.

Space group	IR vibron	Raman vibron	IR phonon	Raman phonon	References
$P6_3/mmc$		A_{1g}		E_{2g}	5,15,16
hcp-c	(0)	(1)	(0)	(1)	
		A_g+T_g	$2T_u$		5,13,14
$Pa3$	(0)	(2)	(2)	(0)	
$P4_2/mnm$		$A_{1g}+B^*_{1g}$	E_u		
rutile	(0)	(2)	(1)	(0)	19
$Pca2_1$	$A_1+B_1+B_2$	$A_1+A_2+B_1+B_2$	$2A_1+2B_1+2B_2$	$2A_1+3A_2+2B_1+2B_2$	19
	(3)	(4)	(6)	(9)	
$P2_1/c$	A_u+B_u	A_g+B_g	$2A_u+B_u$	$3A_g+3B_g$	19
	(2)	(2)	(3)	(6)	
$Pmc2_1$	$A_1+B^*_1$	$A_1+B^*_1$	$A_1+B^*_1$	$A_1+A_2+B^*_1$	18
	(2)	(2)	(2)	(3)	
$P2/m$	B_u	A_g		$2A_g+B_g$	18
	(1)	(1)	(0)	(3)	
$Cmca$		$A_{1g}+B_{3g}$	$B_{1u}+B_{2u}$		21
	(0)	(2)	(2)	(0)	
$P6_3/m$	E_{1u}	$2A_g+E_{2g}$	A_u+2E_{1u}	$2A_g+E_{1g}+3E_{2g}$	23
	(1)	(3)	(3)	(6)	
		Experimental observations for *ortho*-D_2			
LP	0[a]	1[a]		1[b]	26,27,37
BSP	3[a]	1[a]			
D-A	1[a]	1[a]			

[a]This work.
[b]See references.

was observed for hcp symmetry, but it was due to impurity-induced IR activity.[25] In that work the intensity of the IR mode was studied as a function of *ortho-para* concentration. This is an excellent example of why spectra from mixed crystals must be used with great caution in efforts to determine lattice symmetry.

In the LP phase, we have observed one Raman vibron and no measurable IR vibron. One phonon mode has been observed in the LP phase.[26–28] This is consistent with the LP phase having hcp symmetry, a structure which has been determined by x-ray diffraction.[29] In the BSP, three vibrons and one Raman vibron are observed; this rules out the earlier proposal[4] of a $Pa3$ structure, since the $Pa3$ has no IR activity. The $Pca2_1$ has three IR vibrons in agreement with experiment, but four Raman vibrons and nine Raman phonons are expected. Since the $Pca2_1$ structure does not have inversion symmetry, three of the four vibrons are Raman and IR active simultaneously. Their irreducible representations are $A1$, $B1$, and $B2$ are shown in Table I. The fourth vibron with irreducible representation $A2$ is Raman active only. Experimentally, we observed three IR vibrons, but only one Raman vibron. The frequency of this Raman vibron is about 100 cm^{-1} lower than the IR vibrons at a pressure of 50 GPa. Experimentally, three Raman vibrons with the same frequencies as the IR vibrons are not observed. This seems to rule out the space group $Pca2_1$ as the structure of the BSP. On the other hand it is possible that the (unobserved) vibrons may have very low Raman intensity and may not have been observed due to signal-to-noise considerations, as our Raman signal-to-noise ratio was quite low. It would be useful to calculate the intensities of all of these modes. Since $Pa3$ symmetry does not allow IR vibron activity which is experimentally observed, we can rigorously rule out this structure for the BSP.

Consider now the D-A phase, where a single IR vibron and one Raman vibron have been observed. The hcp, $P4_2/mnm$, and $Pa3$ structures are eliminated since they have no IR allowed vibron. The $Cmca$ structure is also eliminated for the same reason. The $P6_3/m$ structure has one distinct IR active vibron, however, the number of allowed Raman vibrons do not match with experiment. For $Pmc2_1$ we expect two IR and two Raman vibrons, as well as three Raman phonons, in disagreement with experiment. The best candidate is the $P2/m$ structure proposed by Kaxiras and Broughton.[18]

In the rest of the paper we shall discuss our data in terms of the $Pca2_1$ and $P2/m$ structures for the BSP and the D-A phase, respectively. This is done to enable some detailed analysis. One should not take this as a statement that we have determined them to be the structures of these phases, rather that they are the proposed structures most consistent with experimental data.

B. Vibron energies for various phases

In the analysis of the vibron excitation energies we follow the theory developed by Van Kranendonk[30] for vibron frequencies in solid hydrogen. In this theory the vibrational potential in a lattice is taken as a sum over the single molecule potentials and a sum over the pair potentials, which can be separated into isotropic and anisotropic parts:

$$V_{\rm tot}=\sum_i V_i^0+1/2\sum_{i\neq j}(V_{ij}^I+V_{ij}^A)\ . \tag{1}$$

Here, V_i^0 is the intramolecular potential; V_{ij}^I and V_{ij}^A are the isotropic and anisotropic intermolecular potentials, respectively. If only the nearest-neighbor (NN) interactions are taken into account, for the hcp structure the two vibrons at $\mathbf{k}=0$ have energies of $\nu_+=\nu_{\rm intra}-3(\varepsilon_1+\varepsilon_2)$ and $\nu_-=\nu_{\rm intra}-3(\varepsilon_1-\varepsilon_2)$, respectively. Here, $\nu_{\rm intra}$ represents the intramolecular interaction energy arising from V_i^0 in Eq. (1), $-\varepsilon_1/2$ is the matrix element of the intermolecular interaction between the vibrational eigenstates of a pair of molecules within the same plane, and $-\varepsilon_2/2$ is that of a pair of molecules in two different planes in an hcp lattice. For an ideal c/a ratio of an hcp lattice [$c/a=\sqrt{(8/3)}$], the in-plane and out-of-plane intermolecular couplings are equal and the two vibron energies reduce to $\nu_+=\nu_{\rm intra}-6\varepsilon$ and $\nu_-=\nu_{\rm intra}$. They correspond to the two molecules in each unit cell vibrating in phase and out of phase, respectively. The former vibration is Raman active, but the latter is IR forbidden because in hcp symmetry the net dipole moment induced in the lattice is zero. However, any equilibrium molecular orientation away from the c axis will lower the hcp symmetry and a net dipole moment will be induced. As a result the IR vibron becomes allowed.

The phase transition from an orientationally ordered structure to a disordered structure can be described by an order parameter. The order parameter provides valuable information for understanding the nature of an order-disordered phase transition. Vibron excitation energies are sensitive to the orientational ordering, and hence can be related to the order parameter. In the following we develop a model which analyzes the vibron excitation energies in the $P2/m$ ad $Pca2_1$ structures. This model allows us to calculate the order parameter from the vibron excitation energies directly and shows how to extract the information from experimental data.

Let us first consider the $P2/m$ structures shown in Fig. 3. Like the hcp space group, this space group also has two molecules in each unit cell. As a consequence there are two vibrational modes, ν_+ with the two molecules vibrating in phase, and ν_- with the two molecules vibrating out of phase. As discussed, the intermolecular couplings in the $P2/m$ symmetry can be split into isotropic and anisotropic contributions. The isotropic interaction between two molecules depends only on the separation of the molecular centers. The anisotropic part can be expanded in spherical harmonics, $Y_{\rm LM}$. It has been shown that at low pressure the anisotropic interaction is dominated by the EQQ interaction.[11] This interaction is responsible for the ordered low-pressure and low-temperature structure of solid molecular hydrogen, the $Pa3$ lattice.[11] Recently, Runge *et al.*,[5] as well as Kaxiras and Guo[31] using local-density approximation electronic-structure calculations, have analyzed the interactions at high density in terms of effective pair interactions. Kaxiras and Guo found a crystal-field-like term which favors

the hexagonal structure and pair interactions in which the most important term transforms as the EQQ interaction. Hence, in the analysis of vibron excitation energies in the high-pressure phases we use an effective EQQ potential. The EQQ-like interaction can be expressed as

$$V_{ij}=V(R)\sum_{M,N}C(224;MN)Y_{2M}(\Omega_i)Y_{2N}(\Omega_j)Y^*_{4,M+N}(\Omega_{ij}) \tag{2a}$$

where $V(R)$ is the radial dependence, $C(224;MN)$ is a Clebsch-Gordon coefficient, and $\Omega_i\equiv(\theta_i,\phi_i)$, Ω_j and $\Omega_{i,j}$ specify, respectively, the orientation of the molecular axes and vector connecting the molecular centers with respect to the crystalline frame. The energy with which a central molecule interacts with its neighbors can be calculated as a function of its orientation.[32] All molecules except the central one are assumed fixed in the equilibrium position. In the calculation we also assume that the orientational distribution of the center molecule is axially symmetric. This simplifies the calculation because we can transform the pair interaction to a coordinate system in which the z axis lies along the equilibrium orientation. Then we average the interaction over the angles in the plane perpendicular to the z axis. If we consider the NN interactions, we find that the orientationally dependent intermolecular interaction for a central molecule in the $P2/m$ structure is

$$V=CY_{20}(\theta)\ . \tag{2b}$$

In this result θ is the polar angle by which the molecular axis deviates from the equilibrium orientation of the $P2/m$ structure. C is a function of the molecular parameters and the lattice constants, hence for a given pressure it is a constant. The anisotropic interaction potential in Eq. (1) can now be replaced by Eq. (2b). Following the Van Kranendonk theory of the vibron frequency in solid hydrogen, the vibron excitation energies at $\mathbf{k}=0$ are then the matrix elements of the vibrational potential of Eq. (1) between the vibrational eigenstates in the solid. The two vibron peak energies of the $P2/m$ structure are expressed as

$$\nu_+=\nu_{\rm intra}-3(\varepsilon_1+\varepsilon_2)-(4\pi/5)^{1/2}\Delta\langle Y_{20}(\theta)\rangle\ , \tag{3a}$$

$$\nu_-=\nu_{\rm intra}-3(\varepsilon_1-\varepsilon_2)-(4\pi/5)^{1/2}\delta\langle Y_{20}(\theta)\rangle\ . \tag{3b}$$

Here $\nu_{\rm intra}$ is the intramolecular vibrational energy; ε_1 and ε_2 are the isotropic intermolecular interactions between the molecules in the same plane and in different planes, respectively. Δ and δ are functions of the molecular parameters and the lattice constants. The last terms in the above equations are the anisotropic interactions and depend on molecular orientations and $\langle Y_{20}(\theta)\rangle$ is a thermal average of the second-order spherical harmonic. When the molecules are disordered, $\langle Y_{20}(\theta)\rangle$ is zero; this corresponds to the disordered LP phase. When the molecules are in the perfect alignment of the $P2/m$ structure, $\langle Y_{20}(\theta)\rangle$ is $(5/4\pi)^{1/2}$. Hence, $\langle Y_{20}(\theta)\rangle$ can be used as an order parameter to describe orientational ordering. The order parameter normalized to one can be defined as $\eta=(4\pi/5)^{1/2}\langle Y_{20}(\theta)\rangle$.

The frequency scaling parameters Δ and δ in Eqs. (3) depend on pressure. In general they also depend on temperature, but in the temperature range we have studied here this can be ignored. For the same reason the temperature dependence of the $\nu_{\rm intra}$, ε_1 and ε_2 can be neglected. Hence, for a given pressure these parameters are the same in both hcp and $P2/m$ structures and the vibron energies in Eqs. (3) can be rewritten as

$$\nu_+(P,T)=\nu_{+\rm dis}(P)-\Delta\eta\ ; \tag{4a}$$

$$\nu_-(P,T)=\nu_{-\rm dis}(P)-\delta\eta\ , \tag{4b}$$

where $\nu_{+\rm dis}$ and $\nu_{-\rm dis}$ are the vibron energies of the disordered LP phase. The significance of these results is that the vibron excitation energies of the ordered phase are direct measures of the order parameter.[7]

Now let us analyze the vibron excitation energies in the $Pca2_1$ structure where the molecules take one of the four orientations shown in Fig. 3. As a consequence, the unit cell in this structure includes four molecules. This lowering in symmetry splits the two vibrons ν_+ and ν_- in the hcp or the $P2/m$ structures into four modes. We consider only the nearest-neighbor interaction and use ε_1 to describe the interaction between two molecules with the same orientation in the same plane and use ε_2 to describe the interaction between the two molecules with different orientations but in the same plane. The interactions between molecules in two different planes are described by ε_3 and ε_4, respectively. Solving the dynamic equations for the four vibrons we get the energies of the vibrons in terms of the intramolecular interaction and the four intermolecular interactions,

$$\nu_1=\nu_{\rm intra}-(\varepsilon_1+2\varepsilon_2+\varepsilon_3+2\varepsilon_4)\ , \tag{5a}$$

$$\nu_2=\nu_{\rm intra}-(\varepsilon_1+2\varepsilon_2-\varepsilon_3-2\varepsilon_4)\ , \tag{5b}$$

$$\nu_3=\nu_{\rm intra}-(\varepsilon_1-2\varepsilon_2+\varepsilon_3-2\varepsilon_4)\ , \tag{5c}$$

$$\nu_4=\nu_{\rm intra}-(\varepsilon_1-2\varepsilon_2-\varepsilon_3+2\varepsilon_4)\ . \tag{5d}$$

All of the four intermolecular interactions can be dissociated into isotropic and anisotropic contributions. Following the analysis in the proceeding section for the $P2/m$ structure, we can rewrite the above equations as

$$\nu_1(P,T)=\nu_{+\rm dis}(P)-\Delta\eta\ , \tag{6a}$$

$$\nu_2(P,T)=\nu_{-\rm dis}(P)-\delta_1\eta\ , \tag{6b}$$

$$\nu_3(P,T)=\nu_{-\rm dis}(P)-\delta_2\eta\ , \tag{6c}$$

$$\nu_4(P,T)=\nu_{-\rm dis}(P)-\delta_3\eta\ . \tag{6d}$$

Here $\nu_{+\rm dis}$ and $\nu_{-\rm dis}$ are the vibron energies of the disordered LP phase, Δ and δ_i, $(i=1,2,3)$ scale the relative shift of the BSP vibrons to the LP vibrons in the disordered phase.

C. Landau theory of second-order phase transitions

Group-theoretical methods can be used to describe phase transitions in crystals, according to Landau

theory.[33] In this theory, a transition is described by an order parameter η. The components of the order parameter η transform like basis functions of an irreducible representation of the space group of the higher symmetry phase. Near the transition, the free energy of the crystal is expanded about $\eta=0$. The space-group symmetry of the crystal requires that only invariant polynomials in this expansion can contribute to the free energy of the crystal. The invariant terms in this expansion determine the nature of the phase transition. If the transition is second order, third degree terms of the form $\eta_i\eta_j\eta_k$ are not allowed to appear in the free-energy expansion. This condition is satisfied if the triplet direct product of the irreducible representation formed by the components of the order parameter η does not contain the identity representation.

The methods have been used by Cullen *et al.*[34] in understanding the phase transition of o-H_2 from the ordered low-temperature phase to the disordered high-temperature phase at ambient pressure. Taking the $Pa3$ structure as the ordered phase and the cubic structure as the disordered phase they have shown that the orientational phase transition from the ordered phase to the disordered phase can not be second order. Considering, in our case, the $P2/m$ structure as the ordered phase and the hcp structure as the disordered high-symmetry phase and taking $\langle Y_{20}(\theta)\rangle$ as the order parameter for the $P2/m$ space group we have arrived at the conclusion that the transition from the $P2/m$ space group to the hcp space group cannot be a second-order transition. Detailed discussion is given in the Appendix.

IV. EXPERIMENTAL RESULTS

The experimental setup and procedure has been described in detail in our recent report on the megabar pressure triple point in solid deuterium.[1] Here the pressure range has been extended to 2.1 Mbar. In the measurements of both the BSP and the D-A phase lines, no thermal hysteresis has been observed. Measurements have been made with increasing pressure, because decreasing pressures in the megabar pressure regime can lead to failure of the diamond anvils.

A. D-A phase

In order to determine the nature of the transition above the triple point, we have measured the temperature dependence of vibron peak frequencies for both the IR and Raman vibrons, as well as the integrated intensity of the IR vibron. The results are shown in Fig. 4(a) for the Raman vibron frequency and in Fig. 5 for the IR vibron integrated intensity and frequency. For comparison we show the temperature dependence of the H-A Raman vibron frequency at a pressure below the triple point in Fig. 4(b) which clearly shows a discontinuity in the vibron frequency. Above the triple point, going from the D-A phase to the LP phase at a constant pressure, the IR vibron integrated intensity gradually decreases to zero. Consistent with the IR vibron integrated intensity, the Raman vibron frequency also continuously changes from

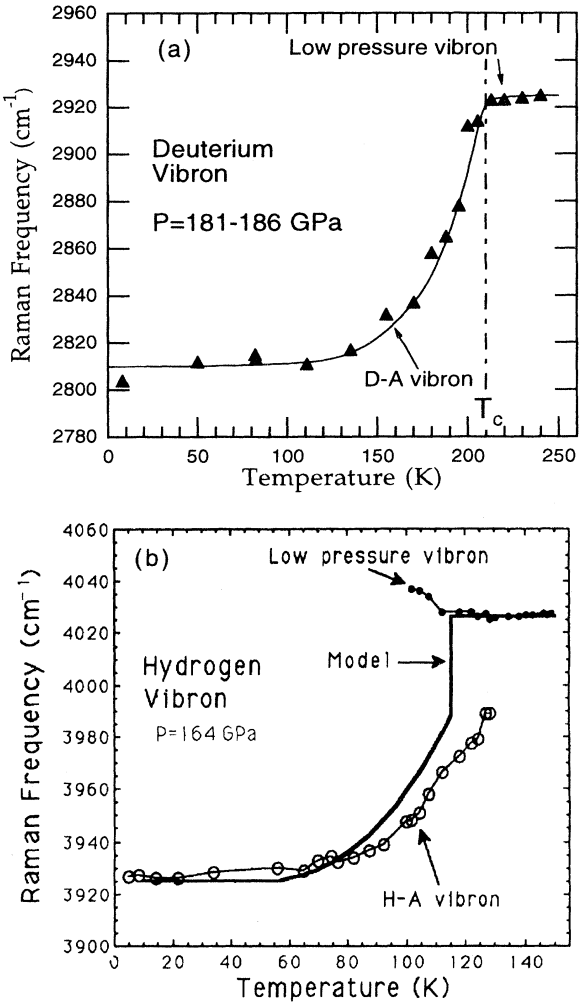

FIG. 4. Raman vibron frequency as a function of temperature (a) for deuterium above the triple point in this work, (b) for hydrogen below the triple point at $P=162$ GPa by Lorenzana, Silvera, and Goettel (Ref. 7). The pressure in (a) was 181 GPa at liquid-helium temperature, however, the pressure drifted to 186 GPa after the temperature cycle of the measurement. The solid line in (a) is a guide to the eye. The solid line in (b) is a computer fitted model for correcting effects due to a pressure distribution (Ref. 7). As discussed in Ref. 7, due to a pressure gradient the LP and the H-A phases coexisted near the H-A phase line. The model with a linear pressure gradient in a sample having a sharply defined transition pressure was used to correct for the distortion.

the low-temperature value in phase D-A to the high-temperature value in phase LP. No discontinuity in the vibron peak frequency is found without our spectral resolution of about 5 cm^{-1}. However, there is a discontinuity in the first derivative of the vibron peak frequency, which is indicated by the kink in Fig. 4(a). The transition temperature determined by the kink is consistent with that determined by the IR vibron integrated intensity. This result means that there is a phase transition even though the discontinuity in the vibron frequency has disap-

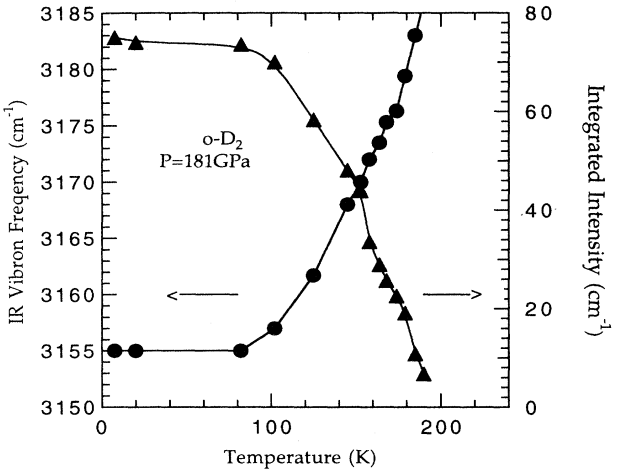

FIG. 5. Temperature dependence of the IR vibron frequency and integrated intensity in the D-A phase at $P=181$ GPa.

peared. This experimental evidence also indicates that the previously reported critical point in hydrogen determined by the disappearance of the discontinuity of Raman vibron frequency[6,7] is insufficient evidence for such a conclusion. We have shown earlier in the analysis of vibron energies, that vibron frequencies can be used as direct measures of the order parameter of the D-A phase. Hence the kink in Fig. 4(a) indicates a second-order phase transition.[33] The integrated intensity of the IR vibron is a direct measure of the order parameter and its square root is proportional to the order parameter as shown by Jochemsen, Berlinsky, and Silvera.[35] The normalized order parameter obtained from the integrated intensity is given in Fig. 6. In Sec. III B we demonstrated that vibron excitation energies are also direct measures of the order parameter. Following the analysis we plot, in Fig. 6, the normalized order parameter from data in Figs. 4(a) and 5 using Eqs. (4). Because the hcp symmetry of the LP phase does not allow IR-active vibrons as discussed in Sec. III A, no IR vibron is observed in the LP phase. In applying Eqs. (4) to extract the temperature dependence of the order parameter, the value $\nu_{-\mathrm{dis}}(P)$ is obtained by extrapolating the low-temperature IR vibron frequency to the transition temperature. The three sets of order parameter data in Fig. 6 are in good agreement.

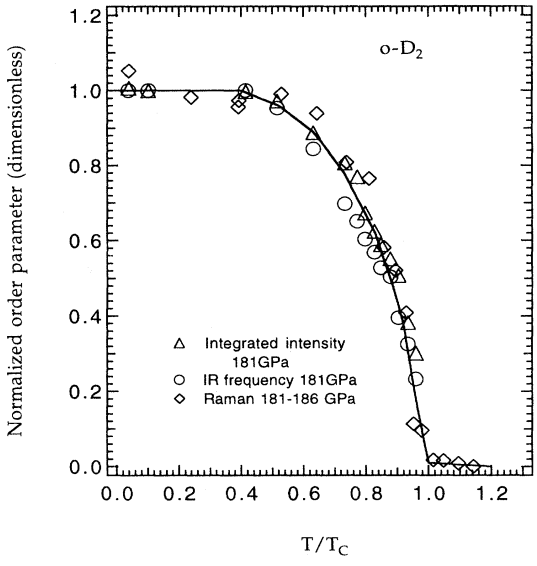

FIG. 6. Normalized order parameter in the D-A phase based on Eqs. (4) and the Raman vibron frequency in Fig. 4(a) and the IR vibron frequency and integrated intensity in Fig. 5. The temperature is normalized to the transition temperature T_c. For the IR frequency data and the corresponding integrated intensity at $P=181$ GPa, $T_c=198$ K is used to normalize the temperature. This number was obtained by extrapolating the integrated intensity in Fig. 5 to zero. For the Raman data at $P=181-186$ GPa, $T_c=210$ K, obtained from Fig. 4(a), is used.

The fact that the experimental order parameter in Fig. 6 continuously changes from unity to zero indicates that the transition from the D-A phase to the LP phase is a second-order phase transition. As a caveat, we note that pressure distribution within the sample can average out a discontinuity in the integrated intensity and make it appear continuous. On the other hand a discontinuity in frequency will not be smoothed out by pressure variations and if it is larger than the experimental resolution it will give a definitive answer. We observed no discontinuity in the frequency.

B. BSP phase

The phase transition from the BSP phase to the LP phase shows a discontinuity in Raman vibron frequency. This discontinuity is a couple of cm^{-1} in D_2 at the transition pressure, 28 GPa.[2] In HD the discontinuity is about 6–7 cm^{-1} at a pressure of 70 GPa,[36] and in H_2 this discontinuity is about 15 cm^{-1} at a pressure of about 110 GPa.

Our IR spectra in the BSP show three vibrons; the integrated intensity of IR vibron 1 and its frequency are plotted in Fig. 7 as a function of temperature at $P=143$

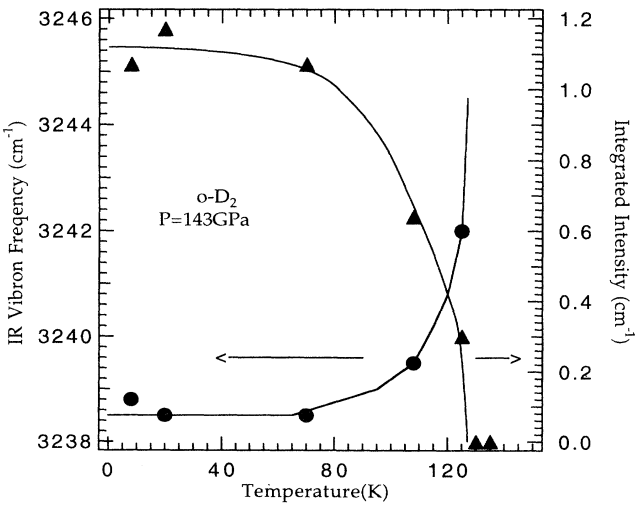

FIG. 7. Temperature dependence of the IR vibron 1 frequency and integrated intensity in the BSP phase at a pressure of 143 GPa.

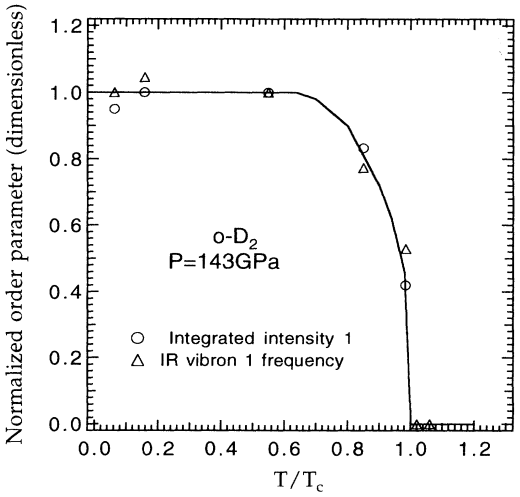

FIG. 8. Normalized order parameter in the BSP phase based on Eqs. (6) and IR vibron frequency and integrated intensity data in Fig. 7. The line is a guide to the eye.

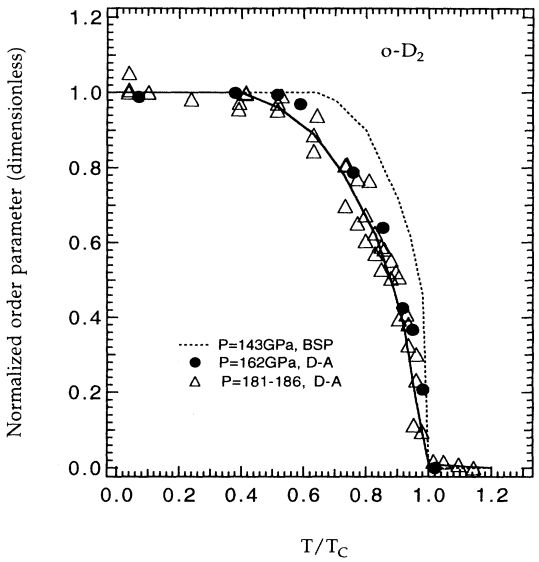

FIG. 9. Comparison of the normalized order parameters at pressures of 162 GPa and 181–186 GPa of the D-A phase and 143 GPa of BSP phase. The curve for the BSP phase is from Fig. 8.

GPa. The integrated intensity decreases with temperature and becomes zero in the LP phase. Like the D-A vibron the BSP vibron also shifts to higher energy with increasing temperature, but the shift from the low-temperature value to the high-temperature value is only several cm^{-1}. In contrast, a similar shift from the low-temperature value of the D-A vibron to the high-temperature value is of order of 30 cm^{-1}. Applying Eqs. (6) to the experimental data of vibron frequency in Fig. 7, we obtain the normalized order parameter η in the BSP phase, shown in Fig. 8. The normalized order parameter obtained from the square root of the integrated intensity of the vibron is also plotted in the same figure. In Fig. 9 we compare the temperature dependence of the order parameters between the BSP and D-A phases in which the normalized order parameters for the D-A phase at the two different pressures are given. From Fig. 9 it is clear that the integrated intensity of the BSP vibron decreases more sharply than that of the D-A vibron. One may argue that a larger pressure gradient in the D-A phase may have smoothed out a sharp transition from the ordered phase to the disordered phase. On the other hand we found that there is no significant trend difference in the experimental order parameters between pressures of 162 and 181 GPa of the D-A phase. This may indicate that the difference in pressure gradients between two pressures differing by 20 GPa is not significant. Hence, the difference in the order parameters between the BSP phase at a pressure of 143 GPa and the D-A phase at a pressure of 162 GPa is unlikely to be due to the difference in the pressure gradients at the two pressures.

C. Pressure dependence of vibrons

Finally, we analyze the pressure dependence of the IR vibron frequency and integrated intensity in the various phases of *ortho*-D_2. The results are shown in Fig. 2 for the peak frequencies and in Fig. 10 for integrated intensities. We observed three peaks in the thick sample (run 1); the two weak peaks were barely resolved. In the thin sample (run 2) the vibron lines were broadened, probably due to more strain. We only observed two peaks in the thin sample, the weaker peak presumably being two unresolved peaks, as we discussed in Ref. 1. We identify the

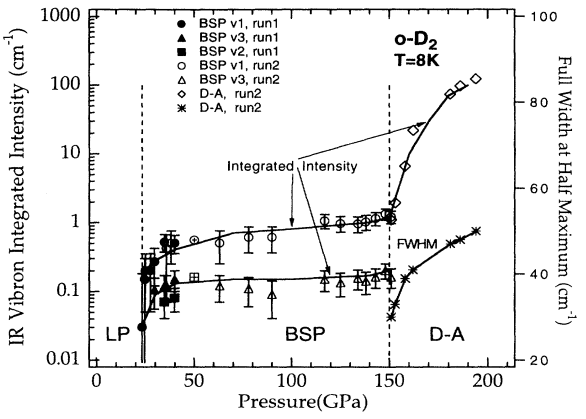

FIG. 10. Pressure dependence of the integrated intensities of the IR vibrons in the various phases of *ortho*-D_2. We believe that the peak represented by the open triangles actually represents vibron $\nu 2$ and $\nu 3$. These peaks are unresolved in run 2 with a thin sample. The solid lines are guides to the eye. The circle and square with crosses inside at 50 GPa represent the numerical results of the integrated intensities of $\upsilon 1$, $\upsilon 2$, and $\upsilon 3$ by artificially splitting the overlapped modes at this pressure. Detailed discussion is given in the text. On the right hand axis we plot the full width at half maximum (FWHM) of the D-A vibron, given by the asterisks.

three vibrons according to their relative intensities. Vibron 1 ($v1$) has the largest integrated intensity as shown in Fig. 10; Vibron 2 ($v2$) has the smallest integrated intensity and vibron 3 ($v3$) is a little bit stronger than $v2$. At about 50 GPa the three vibrons mode frequencies cross, as shown in Fig. 2. Since the three modes cannot be separated at this pressure, the integrated intensity of the peak is actually the sum of the three modes. We numerically split the peak based on the extrapolation of the integrated intensities of $v1$ and unresolved $v3$ and $v2$. The numerical results are given by the circle and square with crosses inside. The large deviation in the $v1$ frequency of run 1 at 48 GPa in Fig. 2 is due to an experimental calibration error in the vibron frequency. The integrated intensities of the vibrons in the BSP phase show a very small pressure dependence. In contrast, the D-A vibron integrated intensity increases with pressure rapidly until it is about two orders of magnitude stronger, within the pressure range we studied. The D-A vibron broadens rapidly with increasing pressure; the line width is also plotted in Fig. 10. Due to a pressure distribution in the sample the BSP and D-A vibrons coexist when the D-A phase is first detected at around 150 GPa. The discontinuity in the vibron frequency clearly indicates a first-order phase transition from the BSP to the D-A phase.

The energy differences between the IR and Raman vibrons at various phases are direct measurements of intermolecular interactions. This can be seen from Eqs. (3)–(6). We have plotted these differences from the experimental data, as shown in Fig. 11 for both the BSP and D-A phases. Our results show discontinuities in these differences at the transition pressure from the BSP to the D-A phase. In hydrogen, Hanfland, Hemley, and Mao[10] reported that the intermolecular interaction is continuous in the transition from the BSP to the H-A phase, based on their IR and Raman data at liquid-nitrogen temperature and concluded that the discontinuity in the Raman and IR vibrons at the transition pressure from the BSP to the H-A phase is attributable to the *intra*molecular interactions. We point out here that their sample was a mixed *ortho-para* crystal so that in their case there was no translational invariance and transitions for all **k** were allowed. As a consequence, the IR vibron peak frequency they measured is probably at the peak of the density of states, whereas their conclusion was based on theory of vibrons at the Brillouin-zone center. The frequency difference between their IR and Raman vibron peaks may not correspond to the intermolecular interaction. A more detailed theory is required to draw conclusions concerning the continuity in the intermolecular interactions in their case. Our results in Fig. 11 indicate that the discontinuities (of order 100 cm^{-1}) in both IR and Raman vibron frequencies in the transition from the BSP to the D-A phase cannot be attributed solely to the *intra*molecular interactions.

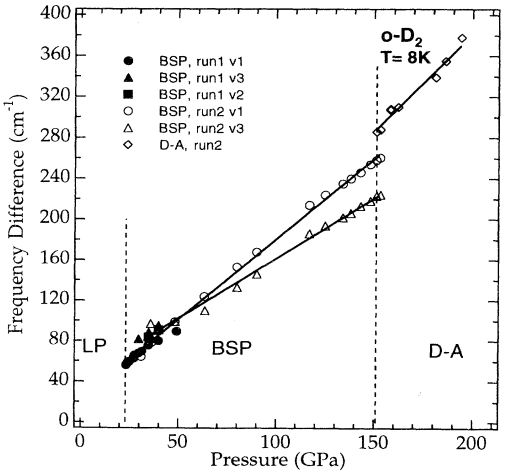

FIG. 11. Frequency difference between IR and Raman vibrons as a function of pressure in the various phases of *ortho*-D_2. The solid lines are linear least-squares fit to the data.

V. CONCLUSIONS

We have presented a detailed data analysis of IR and Raman vibron excitations for both the BSP and the D-A phase. To narrow down the possible structures of the two phases, we have performed a group-theoretical analysis of IR and Raman activity of various vibrational modes for the theoretically proposed high-pressure phases of the hydrogens. According to this analysis, possible candidate structures for the BSP and D-A phases are $Pca2_1$ and $P2/m$, respectively. This result indicates that the underlying molecular centers in both phases form hcp lattices, but the molecules in each phase have different orientational ordering. Based on the above structures we have analyzed the vibron energies in both phases in terms of intramolecular and intermolecular interactions and have shown how the frequencies can be used as a direct measure of the order parameter. The experimentally observed temperature dependence of the IR and Raman vibrons frequencies and integrated intensities were used to determine order parameters in both phases.

From comparison of experimental observations to allowed modes for the D-A phase, the $Pa3$ and hcp structures can be excluded. From this point of view $P2/m$ qualifies as a candidate structure. However, we have used Landau theory to analyze the order of the phase transition from $P2/m$ to hcp for a single order parameter and this is predicted to be first order, not second order, as experimentally observed. Therefore $P2/m$ can be excluded as a candidate structure for the D-A phase. For the BSP phase, the proposed $Pa3$ structure has been excluded. For the model structure $Pca2_1$ the number of observed IR modes agrees with predictions, but more Raman modes are predicted than observed.

We have demonstrated that group-theoretical analysis of IR and Raman-active modes is a powerful tool for determining the structures of the high-pressure phases. Future work in achieving high Raman signal-to-noise ratio should be pursued to search for additional modes with weak intensity. IR and Raman measurements of phonon modes are also valuable. It will also be helpful to theoretically analyze the relative intensities of the vibrational modes for various structures.

ACKNOWLEDGMENTS

We thank E. Kaxiras and W. Evans for helpful discussions. Support from the U.S. Air Force Phillips Laboratory, Contract No. F29601-92-C0019 is gratefully acknowledged.

APPENDIX

Landau theory states that a second-order phase transition from a low-symmetry space group to a high-symmetry space group is driven by the order parameter of the low-symmetry phase. The components of the order parameter in the low-symmetry phase transform like basis functions of an irreducible representation of the space group of the high-symmetry phase. The condition for the second-order phase transition is that the triple direct product of the irreducible representation formed by the components of the order parameter does not contain the identity representation.

In applying the Landau theory to the phase transition from the $P2/m$ space group to the hcp space group, we need to find out the components of the order parameter in the $P2/m$ space group. These components transform like basis functions of an irreducible representation of the hcp space group. The order parameter $\eta=(4\pi/5)^{1/2}\langle Y_{20}(\theta)\rangle$ in the $P2/m$ space group can be represented by one quantity, $3\xi^2-r^2$, where ξ is the projection along the equilibrium molecular axis. Application of the symmetry operations of the high-symmetry hcp space group on $3\xi^2-r^2$ gives rise to the independent components η_i of the order parameter, which forms an irreducible representation of the hcp space group. From the obtained irreducible representation, we can calculate the triple direct product. We find that this contains the identity representation. Hence, the transition from the $P2/m$ space group to the hcp space group cannot be a second-order transition.

[1] L. Cui, N. H. Chen, S. J. Jeon, and I. F. Silvera, Phys. Rev. Lett. **72**, 3048 (1994).
[2] I. F. Silvera and R. J. Wijngaarden, Phys. Rev. Lett. **47**, 39 (1981).
[3] H. E. Lorenzana, I. F. Silvera, and K. A. Goettel, Phys. Rev. Lett. **64**, 1939 (1990).
[4] J. C. Raich and R. D. Etters, J. Low Temp. Phys. **22**, 213 (1972).
[5] K. J. Runge, M. P. Surh, C. Mailhiot, and E. L. Pollock, Phys. Rev. Lett. **69**, 3527 (1992).
[6] R. H. Hemley and H. K. Mao, Science **249**, 391 (1990).
[7] H. E. Lorenzana, I. F. Silvera, and K. A. Goettel, Phys. Rev. Lett. **65**, 1901 (1990).
[8] I. F. Silvera, Sov. J. Low Temp. Phys. **19**, 628 (1993).
[9] R. Zallen, R. N. Martin, and V. Natoli, Phys. Rev. B **49**, 7032 (1994).
[10] M. Hanfland, R. J. Hemley, and H. K. Mao, Phys. Rev. Lett. **70**, 3760 (1993).
[11] I. F. Silvera, Rev. Mod. Phys. **52**, 393 (1980).
[12] J. van Kranendonk, Can. J. Phys. **38**, 240 (1960).
[13] D. E. Ramaker, L. Kumar, and F. E. Harris, Phys. Rev. Lett. **34**, 812 (1975).
[14] C. Friedli and N. W. Ashcroft, Phys. Rev. B **16**, 662 (1977).
[15] T. W. Barbee III, A. Garcia, M. L. Cohen, and J. L. Martins, Phys. Rev. Lett. **62**, 1150 (1989).
[16] A. Garcia, T. W. Barbee III, M. L. Cohen, and I. F. Silvera, Europhys. Lett. **13**, 355 (1990).
[17] E. Kaxiras, J. Broughton, and R. J. Hemley, Phys. Rev. Lett. **67**, 1138 (1991).
[18] E. Kaxiras and J. Broughton, Europhys. Lett. **17**, 151 (1992).
[19] H. Nagara and T. Nakamura, Phys. Rev. Lett. **68**, 2468 (1992).
[20] M. P. Surh, T. W. Barbee, and C. Mailhiot, Phys. Rev. Lett. **70**, 4090 (1993).
[21] B. Edwards and N. W. Ashcroft, Bull. Am. Phys. Soc. **39**, 336 (1994).
[22] M. Surh (private communication).
[23] H. M. James, Phys. Rev. **167**, 862 (1967).
[24] V. Natoli, R. M. Martin, and D. Ceperley, Phys. Rev. Lett. **74**, 1601 (1995).
[25] S. A. Boggs, M. J. Clouter, and H. L. Welsh, Can. J. Phys. **50**, 2061 (1972).
[26] P. J. Berkhout and I. F. Silvera, J. Low Temp. Phys. **36**, 231 (1979).
[27] R. J. Wijngaarden and I. F. Silvera, Phys. Rev. Lett. **44**, 456 (1980).
[28] R. J. Hemley, J. H. Eggert, and H. K. Mao, Phys. Rev. B **48**, 5779 (1993).
[29] H. K. Mao, A. P. Jephcoat, R. J. Hemley, L. W. Finger, C. S. Zha, R. M. Hazen, and D. E. Cox, Science **239**, 1131 (1988).
[30] J. van Kranendonk, *Solid Hydrogen,* 1st ed. (Plenum, New York, 1983).
[31] E. Kaxiras and Z. Guo, Phys. Rev. B **49**, 11 822 (1994).
[32] B. Kohin, J. Chem. Phys. **33**, 882 (1960).
[33] L. D. Landau and E. M. Lifshitz, *Statistical Physics* (Pergamon, New York, 1980).
[34] J. R. Cullen, D. Mukamel, S. Shtrikman, L. C. Levitt, and E. Callen, Solid State Commun. **10**, 195 (1972).
[35] R. Jochemsen, A. J. Berlinsky, F. Verspaandonk, and I. F. Silvera, J. Low Temp. Phys. **32**, 185 (1978).
[36] F. Moshary, N. H. Chen, and I. F. Silvera, Phys. Rev. Lett. **71**, 3814 (1993).
[37] R. J. Hemley, J. H. Eggert, and H. K. Mao, Phys. Rev. B **48**, 5779 (1993).